environmental microbiology

Environmental Microbiology (2016) **18**(6), 2025–2038 doi:10.1111/1462-2920.13226

Environmental drivers of microbial community shifts in the giant barrel sponge, *Xestospongia muta*, over a shallow to mesophotic depth gradient

Kathleen M. Morrow,[1] Cara L. Fiore[1†] and Michael P. Lesser[2*]

[1]*Department of Molecular, Cellular and Biomedical Sciences and*

[2]*School of Marine Science and Ocean Engineering, University of New Hampshire, Durham NH 03824, USA.*

Summary

The giant barrel sponge, *Xestospongia muta*, is a high microbial abundance sponge found on Caribbean coral reefs along shallow to mesophotic depth gradients where multiple abiotic factors change with depth. Sponges were collected along a depth gradient at Little Cayman (LC) and Lee Stocking Island (LSI), and the microbiome of these samples was analysed using 16S rRNA amplicon sequencing. Statistically significant shifts in community structure and dissimilarity (~ 40%) were detected from 10 to 90 m in LC sponges, but a similar shift was not identified in sponges from 10 to 60 m at LSI (only 17% dissimilar). Additionally, inorganic nutrient levels steadily increased with depth at LSI but not at LC. Based on bulk stable isotopic variability, sponges collected from LC were generally more enriched in ^{15}N and less enriched in ^{13}C as depth increased, suggesting a transition from dependency on photoautotrophy to heterotrophy as depth increased. Patterns of stable isotopic enrichment were largely invariant at LSI, which is also reflected in the more stable microbial community along the depth gradient. It appears that environmental factors that change with depth may contribute to differences in *X. muta* microbial assemblages, demonstrating the importance of contemporaneous environmental sampling in studies of the microbiome of sponges.

Received 30 November, 2015; revised 9 January, 2016; accepted 11 January, 2016. *For correspondence. E-mail mpl@unh.edu; Tel. (603) 862 3442; Fax (603) 862 2621. †Current address: Marine Chemistry and Geochemistry, Wood Hole Oceanographic Institute, Woods Hole, MA 02543, USA.

Introduction

Mesophotic coral ecosystems (MCEs) are low-light adapted deep reef communities that range from 30 to 150 m (Lesser *et al.*, 2009). These reefs are typically further offshore from anthropogenic stressors (e.g. coastal development run-off and point-source discharges) and generally below the depth limits of natural stressors (e.g. storm events and thermal effects). As a result MCEs are increasingly recognized as potentially important refugia for a variety of shallow reef species, with broad depth distributions, that have been impacted by these stressors (Lesser *et al.*, 2009; Bongaerts *et al.*, 2010; Slattery *et al.*, 2011; Kahng *et al.*, 2014). While there is evidence that some MCE species have distinct populations along a shallow to deep depth gradient (e.g. the coral *Montastraea cavernosa*; Lesser *et al.*, 2010; Brazeau *et al.*, 2013), there is very little known about microbial communities generally, or the host–microbe interactions of dominant taxa, along the shallow to mesophotic reef depth gradient.

Sponges have emerged as the dominant taxon on many coral reefs (Colvard and Edmunds, 2011; McMurray *et al.*, 2010; van Soest *et al.*, 2012) relative to regional declines in coral cover over the last three decades (Gardner *et al.*, 2003). The ecological importance of sponges to coral reef community structure and function is unambiguous (Wulff, 2006, 2012; Pawlik, 2011). Sponges provide important food and habitat for a variety of coral reef species (e.g. Randall and Hartman, 1968; Diaz and Rutzler, 2001), and they can both stabilize or degrade the reef matrix with the associated implications for the community (Wulff, 1984; Bell, 2008). In addition, sponges host diverse assemblages of symbiotic microorganisms (Hentschel *et al.*, 2012; Taylor *et al.*, 2007; Thacker and Freeman, 2012; Morrow *et al.*, 2014). Many of these microbes form specific and stable associations (e.g. Reveillaud *et al.*, 2014) and are major contributors to carbon, nitrogen, phosphorous and silica cycling in coral reef ecosystems (Corredor *et al.*, 1988; Mohamed *et al.*, 2008; Southwell *et al.*, 2008; Fiore *et al.*, 2010; 2013a; Maldonado *et al.*, 2012; Zhang *et al.*, 2015). Sponges and/or their symbiotic microbial communities also produce critical secondary metabolites that play important roles in deterring predators (Pawlik, 2011;

Slattery and Gochfeld, 2012). Sponges are also important competitors with corals and algae (Lopez-Victoria *et al*., 2006) where experimental evidence shows that their success is due to chemical defences (Porter and Targett, 1988; Pawlik, 2011; Slattery and Gochfeld, 2012; but see Slattery and Lesser, 2014). Many sponge species in the Caribbean span the gradient of shallow to deep reefs (Fiore *et al*., 2013a,b; Olson and Gao, 2013; Slattery *et al*., 2015), providing an ideal opportunity to study changes in the microbial ecology of the sponge microbiome along the shallow to mesophotic depth gradient (Olson and Kellogg, 2010).

Xestospongia muta is an important member of sponge communities on both shallow and mesophotic reefs in the Caribbean and is classified as a high microbial abundance (HMA) bacteriosponge. It harbours both *Proteobacteria* and *Cyanobacteria* as members of its microbiome, with the potential for nitrogen fixation, as well as nitrate and nitrite reduction (Fiore *et al*., 2010; 2013a,b; 2015; Olson and Gao, 2013). Here we describe the changes in the microbiome of *X. muta* from shallow to mesophotic depths in a 16S rRNA gene-targeted metagenetic approach at two locations in the Caribbean: Lee Stocking Island, Bahamas, and Little Cayman, Cayman Islands. This sequencing effort combined with measurements of relevant environmental factors will help us assess whether *X. muta* microbiome community structure and stability vary as a result of changing external factors across the mesophotic depth gradient at either site.

Results

Midday vertical profiles of photosynthetically active radiation (PAR) showed little variability (± 5–10%) during the experimental period, suggesting that the optical properties of the water column changed very little during this time period at any given depth. Vertical profiles of PAR for Little Cayman (LC) and Lee Stocking Island (LSI) had maximum surface irradiances ranging from 2215 to 2445 μmol quanta m^{-2} s^{-1} (Fig. 1A). The mean K_{dPAR} for the water column ranged from 0.056 to 0.057 m^{-1}, with the 10% optical depth (mid-point of euphotic zone) occurring at 40–41 m (112–106 μmol quanta m^{-2} s^{-1}) and the 1% optical depth (= compensation depth or bottom of euphotic zone) occurring at 81–82 m (10–19 μmol quanta m^{-2} s^{-1}) for LC and LSI respectively. Vertical profiles (Fig. 1B) of temperature showed a well-mixed water column down to approximately 25 m at LC and ~ 50 m at LSI, with changes in temperature from 28.8–29.3°C at the surface to 24.8–25.4°C at 91 m respectively. Nutrient (NOx) concentrations as a function of depth (Fig. 1C) were not significant for LC (analysis of variance [ANOVA]: $F = 0.121$, $P = 0.946$), while the NOx was significantly different across the depth gradient at LSI (Fig. 1C; ANOVA: $F = 3.652$, $P = 0.039$). Multiple comparison testing revealed that the Shallow depths were significantly different (Tukey's HSD (honest significant difference) test $P < 0.05$) to the Very Deep Depths, and there was significant overlap with Medium and Deep depth NOx concentrations (Fig. 1C). The analysis of the bulk stable isotope data showed (Fig. 1D) that the sponges from LC became less depleted in their $\delta^{13}C$ values with depth (ANOVA: $F = 6.963$, $P = 0.004$), as did LSI (ANOVA: $F = 4.396$, $P = 0.022$), while there was no significant effect of depth for the $\delta^{15}N$ signatures at LC (ANOVA: $F = 2.561$, $P = 0.097$) or LSI (ANOVA: $F = 1.505$, $P = 0.257$). Both locations follow a general trend of samples grouping together according to depth driven by their $\delta^{13}C$ values (Fig. 1D).

Pyrosequencing of the 16S rRNA gene recovered a total of 109 249 reads from samples collected at LC, with an average of 1750 ± 412 SE (standard error) reads per sample, ranging from 5152 ± 325 SE (45 m) to 7521 ± 1446 SE (10 m; Table 1). At LSI, a total of 114 565 reads were recovered, with an average of 6364 ± 595 reads per sample, ranging from 4591 ± 118 (23 m) to 10 360 ± 1772 (60 m; Table 1). A total of 530 unique operational taxonomic units (OTUs) were retrieved from LC and 548 OTUs from LSI sponge samples, including 30 unique phyla across both sites. Microbial community structure based on 16S rRNA amplicons differed significantly between depth ranges at both LC (permutational analysis of variance [PERMANOVA]: $F = 3.18$, $P = 0.001$) and LSI (PERMANOVA: $F = 1.84$, $P = 0.02$). At LC, depth range was a significant driver of microbial community structure between all ranges, except 'shallow versus medium' and 'medium versus deep' zones (Fig. 2; Table S1). Microbial community changes in Very Deep LC samples affiliate with depth in addition to $\delta^{13}C$ and $\delta^{15}N$ signatures, which are opposed to community changes in Shallow samples that are affiliated with light (irradiance) and temperature measurements (Fig. 3). Nutrient (NOx) measurements appear to drive microbial community changes in samples collected at the Deep LC site based on canonical correspondence analysis (CCA) vectors (Fig. 3). Similarity percentage analysis (SIMPER) demonstrated a ~ 38% dissimilarity between Shallow (10 m) and Very Deep (91 m) samples (Table S2). Based on the multivariate generalized linear model (MGLM) analysis using *mvabund*, dissimilarity was driven largely by a significant decline ($P < 0.05$) in the relative abundance of OTUs related to the families *Rhodobacteraceae* (Cl. *Alphaproteobacteria*) and *Synechococcaceae* (Ph. *Cyanobacteria*), which are both potential photosymbionts (Fig. 4, Table 1, Table S2). As depth increased there was also significant decline in the relative abundance of the family *Rhodothermaceae* (Ph. *Bacteroidetes*), coupled with the appearance of OTUs related to the family

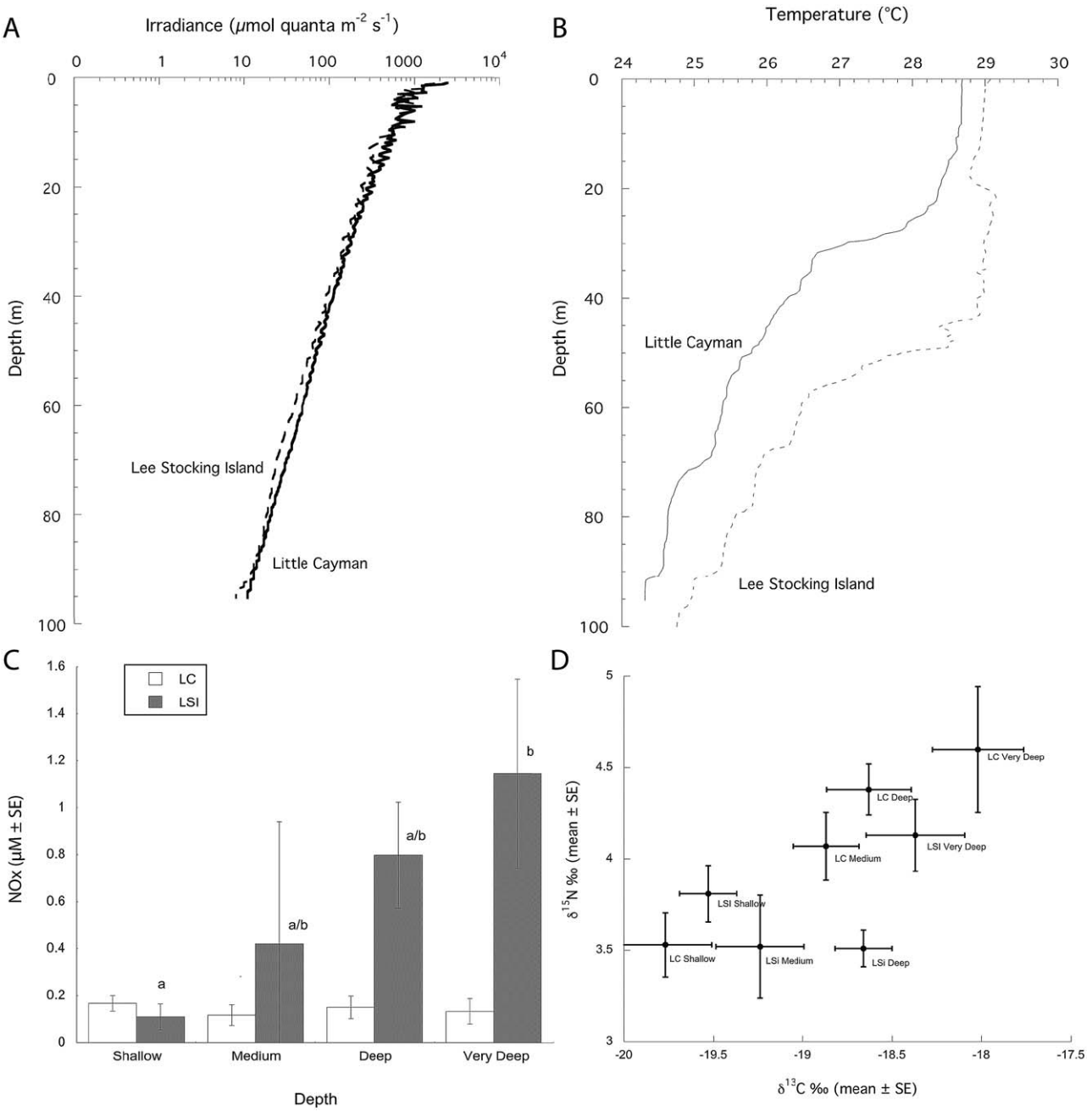

Fig. 1. Vertical profiles of environmental parameters collected at Little Cayman (LC) and Lee Stocking Island (LSI) at 10–60 m and 10–91 m respectively.
A. Downwelling (E_d) photosynthetically active radiation (PAR: 400–700 nm).
B. Temperature (°C); nutrient (NOx) concentrations as a function of depth.
D. Bulk stable isotope data for $\delta^{13}C$ and $\delta^{15}N$ from *Xestospongia muta* sponges collected at each depth range (Shallow = 10 m, Medium = 15–23 m, Deep = 30–46 m and Very Deep = 60–91 m).

Entotheonellaceae (Cl. *Deltaproteobacteria*) at 60 and 90 m depths (Table 1, Table S2). Sequences affiliated with *Synechococcus* sp. were the most abundant OTUs from 10 to 46 m (~ 10–24% of the total microbiome), replaced by OTUs affiliated with the phylum *Chloroflexi* at 60 m. The relative abundance of phyla often found in association with bacteriosponges (i.e. *Chloroflexi* and *Poribacteria*) increased with depth at LSI, as did the relative abundance of *Ectothiorhodospiraceae* (Cl. *Gammaproteobacteria*; Fig. 4, Table 1). The *Ectothiorhodospiraceae* also photosynthesize and prefer an anaerobic environment, as they are members of the

Table 1. Number of sequences retrieved and relative abundance of top 10 operational taxonomic units (OTUs) at each depth zone.

(A) Little Cayman					10 m	18 m	30 m	46 m	60 m	91 m
Average reads after quality filtering ± SE per depth					7521 ± 1447	6779 ± 1068	7027 ± 1085	5152 ± 325	5183 ± 727	5413 ± 115
Archaea	Class	Order	Family	Genus	10 m	18 m	30 m	46 m	60 m	91 m
Crenarchaeota	*Thaumarchaeota*	*Cenarchaeales*	*Cenarchaeaceae*	*Nitrosopumilus*	1.0	2.5	6.9	3.2	3.3	6.6
Bacteria	Class	Order	Family	Genus	30	60	100	150	200	300
Acidobacteria	*Acidobacteria*	*BPC015*	Unclassified			1.2		1.1	1.8	1.1
		iii1-15	Unclassified			1.3		1.2	2.9	3.2
	Solibacteres	*Solibacterales*	PAUC26							
Actinobacteria	*Acidimicrobiia*	*Acidimicrobiales*	Unclassified		1.8	1.9	6.2	2.8	1.9	3.0
			TK06/ wb1_P06		1.1	1.1	2.2	1.2		3.1
Bacteroidetes	*Rhodothermi*	*Rhodothermales*	*Rhodothermaceae*		6.0	1.4	1.8	2.9		1.4
Chloroflexi	*Anaerolineae*	*Caldilineales*	*Caldilineaceae*			1.4	1.3	1.4	3.0	3.2
	Anaerolineae	SBR1031	A4b				1.0	1.5	1.1	1.4
	SAR202	Unclassified	Unclassified		2.9	7.7	4.1	9.0	14.8	7.9
Cyanobacteria	*Synechococcophycideae*	*Synechococcales*	*Synechococcaceae*	*Synechococcus*	23.8	17.2	10.2	14.6	7.0	9.4
Gemmatimonadetes	*Gemm-2*	Unclassified	Unclassified		0.9		2.3	1.3	1.6	1.8
PAUC34	Unclassified	Unclassified	Unclassified							
Planctomycetes	*Brocadiae*	*Brocadiales*	*Brocadiaceae*	*Candidatus Jettenia*	4.0					
Poribacteria	Unclassified	Unclassified	Unclassified		2.7	4.3	3.2	6.6	10.0	7.0
Proteobacteria										
	Alphaproteobacteria	*Rhodobacterales*	*Rhodobacteraceae*		9.8	5.7	3.8	4.0	1.0	
		Rhodospirillales	*Rhodospirillaceae*		2.0	1.6	1.0	1.8	2.4	2.3
	Deltaproteobacteria	*Entotheonellales*	*Entotheonellaceae*					0.9	2.2	2.3
		Spirobacillales	Unclassified		1.2					
		Syntrophobacterales	*Syntrophobacteraceae*			1.5		1.5	3.0	1.6
	Gammaproteobacteria	*Alteromonadales*	HTCC2188	HTCC	5.1	2.4	6.7	5.2		2.6
		Chromatiales	Unclassified		3.3	1.9	3.9	2.9	3.6	5.2
		Chromatiales	*Ectothiorhodospiraceae*			0.9	1.0	1.5	2.3	2.8
		HTCC2188	HTCC2089		14.5	13.1	6.3	13.6	6.9	3.2
		Oceanospirillales	Unclassified			4.2				
		Oceanospirillales	*Endozoicimonaceae*							
		Thiotrichales	*Piscirickettsiaceae*		1.5		9.2	2.4	2.1	3.6
		Vibrionales	*Pseudoalteromonadaceae*	*Pseudoalteromonas*		4.6				
		Unclassified	Unclassified		1.2	1.4	3.2	2.1		
Spirochaetes	*Spirochaetes*	*Spirochaetales*	*Spirochaetaceae*						1.0	1.5
Unassigned					7.2	5.4	8.2	8.1	7.3	11.0

Table 1. *cont.*

(B) Lee Locking Island					10 m	15 m	23 m	30 m	46 m	60 m
Average reads after quality filtering ± SE per depth					5747 ± 589	5677 ± 225	4591 ± 118	5369 ± 1816	5874 ± 1009	10 360 ± 1771
Archaea	Class	Order	Family	Genus	10 m	15 m	23 m	30 m	46 m	60 m
Crenarchaeota	*Thaumarchaeota*	*Cenarchaeales*	*Cenarchaeaceae*	*Nitrosopumilus*	3.0	2.4	2.3	4.1	2.7	3.3
Bacteria	Class	Order	Family	Genus						
Acidobacteria	*Acidobacteria*	*BPC015*	Unclassified		1.9		1.4		2.0	1.3
		iii1-15	Unclassified		3.0	1.5	3.8	1.9	3.3	3.2
	Solibacteres	*Solibacterales*	PAUC26		2.3		2.2	1.0	1.7	1.6
Actinobacteria	*Acidimicrobiia*	*Acidimicrobiales*	Unclassified		2.7	3.1	2.1	2.5	2.1	2.3
			TK06/ wb1_P06			1.1	1.1			
Bacteroidetes	*Rhodothermi*	*Rhodothermales*	*Rhodothermaceae*		2.6	3.2	4.4	2.2	1.0	1.7
Chloroflexi	*Anaerolineae*	*Caldilineales*	*Caldilineaceae*		2.2	1.8	2.2	2.4	3.1	2.4
	Anaerolineae	*SBR1031*	A4b		1.2					
	SAR202	Unclassified	Unclassified		12.6	6.1	11.0	10.6	12.1	13.1
Cyanobacteria	*Synechococcophycideae*	*Synechococcales*	*Synechococcaceae*	*Synechococcus*	4.7	11.2	8.3	9.7	4.1	3.1
Gemmatimonadetes	*Gemm-2*	Unclassified	Unclassified		3.5	1.8	1.7	1.8	2.0	2.0
PAUC34	Unclassified	Unclassified	Unclassified		2.6	2.3	2.8	2.9	4.2	3.0
Planctomycetes	*Brocadiae*	*Brocadiales*	*Brocadiaceae*	*Candidatus Jettenia*				1.5		1.6
Poribacteria	Unclassified	Unclassified	Unclassified		9.6	4.9	6.7	8.6	12.0	9.9
Proteobacteria										
	Alphaproteobacteria	*Rhodobacterales*	*Rhodobacteraceae*		2.8	5.5	5.0	4.1	1.1	1.9
		Rhodospirillales	*Rhodospirillaceae*		4.7	2.5	3.5	2.0	3.9	2.9
	Deltaproteobacteria	*Entotheonellales*	*Entotheonellaceae*		1.6		1.3	1.5	1.9	1.6
		Spirobacillales	Unclassified							
		Syntrophobacterales	*Syntrophobacteraceae*		2.0	1.7	2.3	3.0	3.1	2.9
	Gammaproteobacteria	*Alteromonadales*	HTCC2188	HTCC	1.6	1.3	1.7	2.5	1.9	
		Chromatiales	Unclassified		3.8	2.3	3.5	2.3	2.6	3.3
		Chromatiales	*Ectothiorhodospiraceae*		2.4	1.0	2.1	2.2	2.9	2.0
		HTCC2188	HTCC2089		7.2	10.5	9.7	9.3	8.5	11.2
		Oceanospirillales	Unclassified					1.0		
		Oceanospirillales	*Endozoicimonaceae*			4.8				
		Thiotrichales	*Piscirickettsiaceae*		1.5	1.7		0.9	1.2	1.5
		Vibrionales	*Pseudoalteromonadaceae*	*Pseudoalteromonas*		1.3				
		Unclassified	Unclassified				1.0			1.0
Spirochaetes	*Spirochaetes*	*Spirochaetales*	*Spirochaetaceae*		1.1	1.0	1.3	1.4	1.5	1.2
Unassigned					6.3	8.5	5.3	9.7	7.7	9.4

Top five most abundant OTUs are indicated with heat map colouration. Key: (▬) Top OTUs; (▬) 2nd; (▬) 3rd; (▬) 4th; (▬) 5th.

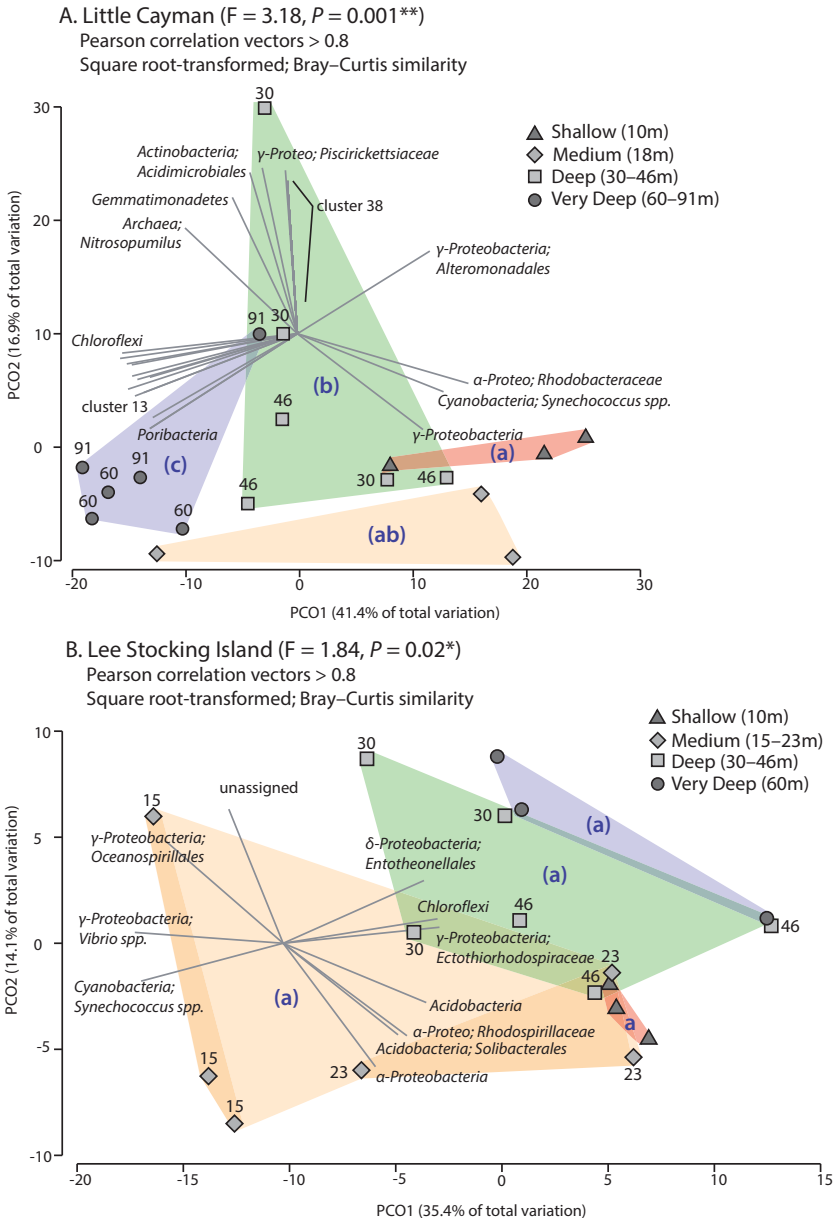

Fig. 2. Principal coordinate analysis (PCoA) plots based on square root-transformed Bray–Curtis distances for each *Xestospongia muta* sample collected within four depth ranges at (A) LC and (B) LSI. Bacterial communities sampled at each depth range: Shallow (red triangles), Medium (orange diamonds), Deep (green squares) and Very Deep (blue circles). Pearson correlation vectors represent the most resolved taxonomy for bacterial OTUs that may be driving dissimilarity between ranges. Pseudo-F and *P*-values are based on PERMANOVA tests. Statistical significance ($P < 0.05$) for pairwise comparisons is illustrated with letters a, b and c. The list of taxa composing OTU clusters 13 and 38 can be found in Table S3.

purple sulfur bacteria within the order *Chromatiales*. Sequences affiliated with the phylum *Bacteroidetes* and class *Alphaproteobacteria* (f. *Rhodobacteraceae* and *Rhodospirillaceae*) demonstrated a general decline in relative abundance from shallow to deep depth zones (Fig. 4, Table 1). Despite depth being a significant factor influencing the relative abundance of members of the sponge microbiome at LC, the core members of the community remained relatively stable across the depth gradient, with < 50% dissimilarity between any two depth ranges (Fig. 4, Table S2).

At LSI, depth range was also a significant driver of overall microbial community changes, but did not drive significant differences between any pairwise comparisons between depth ranges (Fig. 2, Table S1). Similar to LC, microbial community changes in Very Deep and Deep LSI samples affiliate with depth in addition to $\delta^{13}C$, $\delta^{15}N$ and nutrient (NOx) signatures based on CCA vectors (Fig. 3). Light (irradiance) and temperature measurements are more highly affiliated with shifts in community structure at Shallow and Medium depths at LSI (Fig. 3). Nutrient (NOx) measurements appear to drive microbial community changes in samples collected at the Deep LC site (Fig. 3). The LSI microbiome was dominated by only a handful of sequence OTUs; for example, the class *Gammaproteobacteria* (HTC2089) demonstrated a consistent pattern of relative abundance across the entire depth gradient (Fig. 4, Table 1). Sequences related to the

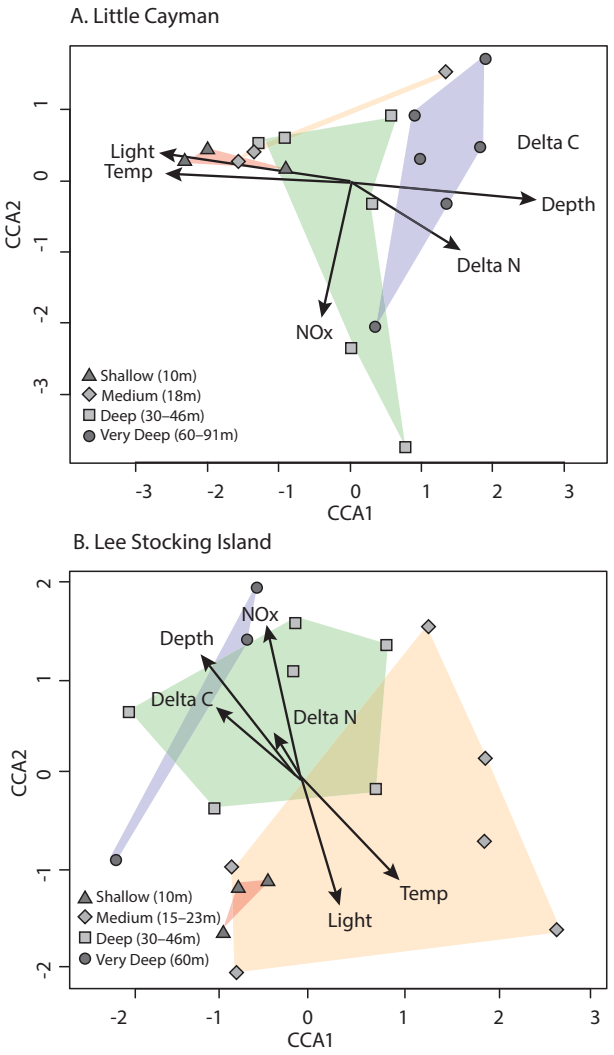

Fig. 3. Canonical correspondence analysis (CCA) ordination plots of 16S rRNA metagenetic *X. muta* microbial communities defined by the first and second axes recorded for (A) Little Cayman at Shallow (red triangles), Medium (orange diamonds), Deep (green squares) and Very Deep (blue circles) depths, and (B) Lee Stocking Island at Shallow (red triangles), Medium (orange diamond), Deep (green squares) and Very Deep (blue circles) depths. Vectors represent environmental variables: light (PAR 400–700 nm), temperature (°C), nutrients (NOx), and bulk stable isotope data for Delta C ($\delta^{13}C$) and Delta N ($\delta^{15}N$).

phyla *Poribacteria* and *Chloroflexi* within the classes SAR202 and *Anaerolineae* were also abundant and consistently represented within the *X. muta* microbiome across the entire depth gradient at LSI. In fact, sequences affiliated with the *Chloroflexi* (SAR202) were the most abundant members of the microbiome across the entire depth gradient (~ 6–13% of the total microbiome), except at 10 m (Medium depth), where sequences affiliated with *Synechococcus* spp. were the dominant members (Table 1). This is in contrast to LC, where the most abundant members of the microbiome were affiliated with *Synechococcus* spp. across the entire depth gradient, except at 60 m, where *Chloroflexi*-related sequences were again the dominant members (Table 1). Sequences affiliated with *Synechococcus* spp. also decreased from 24% to 9% of the total sponge microbiome at LC, but were considerably less variable across the depth gradient at LSI than LC (Fig. 4, Table 1). These photosynthetic populations are likely responding and adapting their nutrient acquisition to the 100-fold decline in irradiance from 10 to 60 m (Fig. 1A).

Discussion

Sponges represent a dominant functional group on coral reefs worldwide, and there is evidence that sponge abundance and biomass are increasing on shallow reefs as coral cover has declined due to anthropogenic stressors (Aronson *et al.*, 2002; McMurray *et al.*, 2010; Bell *et al.*, 2013). Additionally, sponge biomass and diversity increases with depth into the mesophotic zone (Lesser *et al.*, 2009), due in part to several factors, including increasing particulate organic carbon, primarily as picoplankton (Lesser, 2006; Lesser and Slattery, 2013), to changes in abiotic factors along the shallow to mesophotic gradient (Lesser *et al.*, 2009), and possibly due to site- or depth-specific differences in predation (Slattery *et al.*, 2015). Recent observations suggest that there is a distinct faunal break at 60 m, where a change in the biodiversity and dominance of sponges occurs (e.g. Reed and Pomponi, 1997). Similarly, the genetic structure and function of corals along shallow to mesophotic gradients appear to exhibit a significant change at 60 m (Bongaerts *et al.*, 2010; Lesser *et al.*, 2010; Brazeau *et al.*, 2013), driven largely by differences in the community composition of their algal symbionts in the genus *Symbiodinium* and the transition from photoautotrophy to heterotrophy of the holobiont (Lesser *et al.*, 2010). Few have examined whether sponges exhibit similar depth-dependent changes in their microbiome.

The giant barrel sponge, *Xestospongia muta*, is an HMA bacteriosponge that supports a diverse community of bacteria that varies in structure across a mesophotic depth gradient. The microbiome of *X. muta* also includes a core group of representatives from the phyla *Chloroflexi*, *Cyanobacteria* (*Synechococcus* spp.), *Bacteroidetes*, *Proteo-*, *Actino*, *Acido-* and *Poribacteria*, as well as Archaea within the genus *Nitrosopumilus* in the phylum *Thaumarchaeota*. Highest diversities within phyla were represented by the *Proteobacteria* (including 74 families), *Actinobacteria* (17 families) and *Bacteroidetes* (11 families), groups that are often dominant members of sponge microbiomes (Schmitt *et al.*, 2012). This community has the potential to play an important role in carbon and nutrient cycling, including but not limited to nitrogen

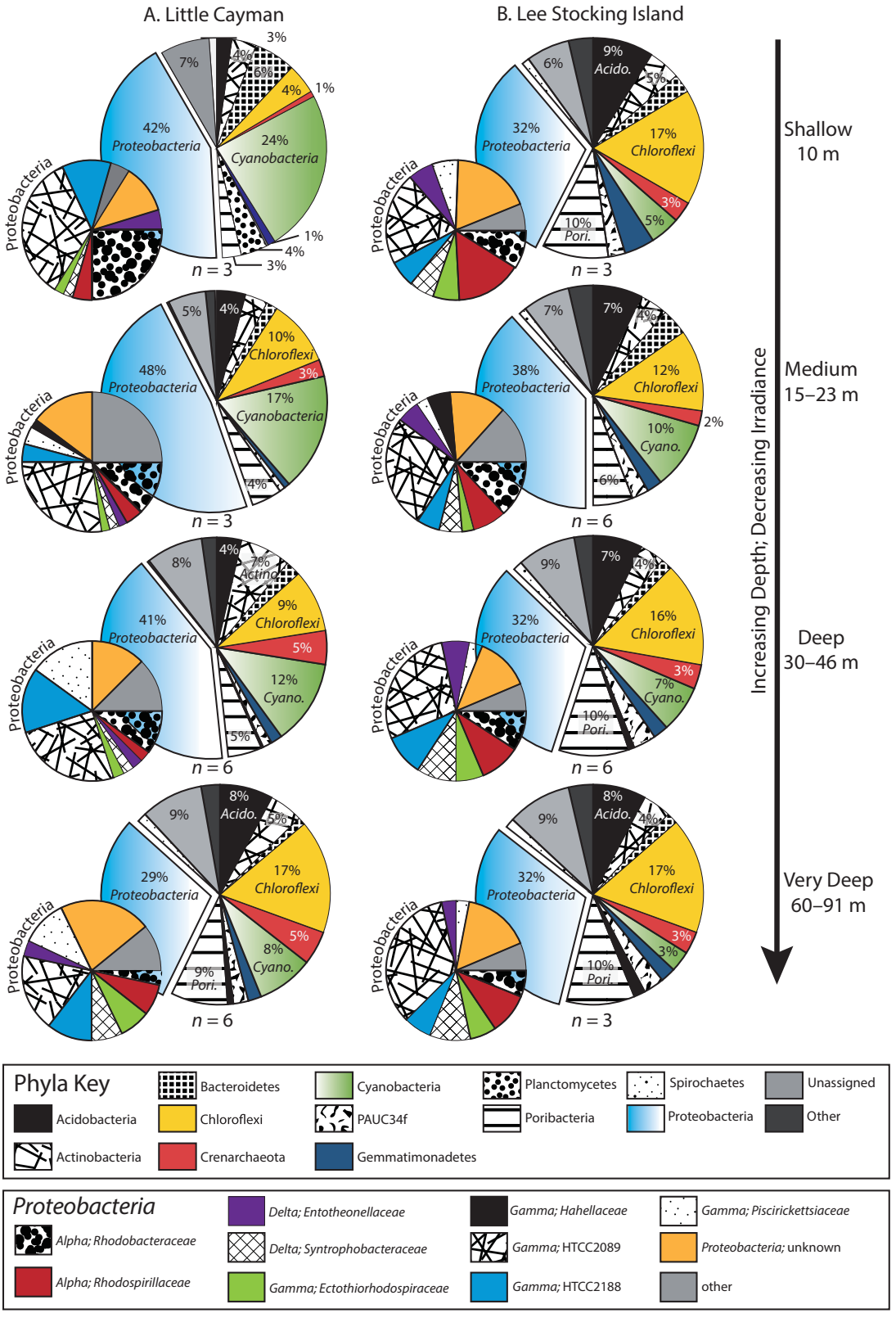

Fig. 4. Pie charts representing average percentage contribution of the most dominant prokaryotic phyla (large pies) to the total relative abundance in *Xestospongia muta* at (A) LC and (B) LSI are presented. *n* = the total number of individual *X. muta* sponges sampled for each depth range at each site. Additionally, all *Proteobacteria* families (small pie charts) are presented across all species replicates for each depth range (Shallow, Medium, Deep and Very Deep).

fixation, nitrate/nitrite reduction, methylotrophy and chemolithotrophic ammonia oxidation (Fiore *et al*., 2013a,b; 2015; Olson and Gao, 2013). Although *X. muta* appears to support a core community of resident microbes, environmental parameters that change with depth facilitate shifts in abundance of certain core phyla that may impact several functional aspects of sponges. Higher levels of nutrients and upwelling at LSI appear to support a more stable microbiome in comparison to LC, where gradients in light and temperature, but not nutrients, drive significant changes in photoautotrophic *Cyanobacteria* in the genus *Synechococcus*, which have been shown to supply a significant amount of carbon to their host via autotrophy in other species of sponges (Wilkinson, 1983; Erwin and Thacker, 2008a). Sequences affiliated with *Synechococcus* spp. are well-described symbionts of *X. muta* (Fiore *et al*., 2013a), which has been shown to harbour different phylotypes of *Synechococcus spongiarum* (Erwin and Thacker, 2008b). Additionally, a study on *X. muta* using isotopic tracers (e.g. $NaH^{13}CO_3$) showed that the bacterial community does readily fix carbon and may translocate labelled products to the host (Fiore *et al*., 2013b). Cyanobacteria demonstrated a decline along the shallow to mesophotic depth gradient at LC while a similar pattern was not evident at LSI, although similar gradients in downwelling irradiance were present. Despite the strong general dependency of cyanobacteria on light, the nitrogen requirements of cyanobacteria in the genus *Synechococcus* are generally high (Lindell *et al*., 2005) such that the increasing NOx concentrations with increasing depth at LSI (Fig. 1C) should be able to support more *Cyanobacteria* within the constraints of the changing mesophotic irradiances. What we observe instead is invariant abundance of *Cyanobacteria* with depth and much higher, but invariant, abundance of *Chloroflexi* with depth at LSI compared with LC. One possibility is that the members of the phylum *Chloroflexi* observed here are photoautotrophic and competing with cyanobacteria for resources (e.g. inorganic carbon) as reported for these taxa in microbial mats at hot springs (Liu *et al*., 2011), but their consistent pattern in relative abundance across the entire depth range suggests that they are taking advantage of another source of nutrients at LSI other than photoautotrophy.

Symbionts in the phyla *Chloroflexi* and *Poribacteria* are diverse and often abundant members of HMA sponges, in comparison to LMA sponges (Hochmuth *et al*., 2010; Schmitt *et al*., 2011). Both are believed to play significant roles in the production of secondary metabolites with a broad range of biological activity, including non-ribosomal peptides (Siegl and Hentschel, 2010), polyketides and methyl-branched fatty acids (Hochmuth *et al*., 2010). Recent genetic sequencing revealed that *Poribacteria* are mixotrophs, undertaking autotrophic carbon fixation via the Wood–Ljungdahl pathway (Siegl *et al*., 2011), in which carbon dioxide is converted through a series of reactions into acetyl-coenzyme A, an important molecule in metabolism and energy production. Thus, endosymbiotic sponge associates such as *Chloroflexi* and *Poribacteria* may play critical roles in both host defence and nutrient acquisition, likely utilizing additional energy sources as photoautotrophy becomes less optimal with increasing depth. Even at shallow depths, LSI *X. muta* sponges support a lower relative abundance of cyanobacterial symbionts than LC sponges, potentially making their microbiomes less reliant on irradiance and more capable of utilizing higher NOx with increasing depth. The gradient from shallow to mesophotic reefs provides a range of important selective forces such as irradiance, nutrient availability and food availability on the resident organisms (Lesser *et al*., 2009; Kahng *et al*., 2014), including their microbiomes (Olson and Kellogg, 2010). These results suggest that the field of environmental microbiology would benefit from synchronous studies that target multiple locations and habitats prior to drawing organism or ecosystem-wide conclusions.

In a comparative study, Olson and Gao (2013) used terminal restriction fragment length polymorphism [T-RFLP] in addition to a limited number of clone libraries (one from each species at a single depth: 45 m), to examine the microbial community structure of three sponge species, including *X. muta*, across a 9 to 90 m depth gradient at LC. The samples examined in Olson and Gao (2013) are from the same *X. muta* sponges collected in the present study, so a direct comparison is relevant. This was the first study to suggest that *X. muta* was a bacteriosponge that supports a diverse community of bacteria, distinct from the water column. As with the current study and previous studies (Steindler *et al*., 2005), *X. muta* was found to support a specific cyanobacterial community, and consistent populations of the phylum *Chloroflexi*, across the depth gradient (Olson and Gao, 2013). Furthermore, although members of the *Actinobacteria* were previously suggested to dominate the microbiome of *X. muta*, making up to 12% of the community based on clone libraries (Montalvo *et al*., 2005), Olson and Gao (2013) suggested they were less abundant members (~ 4.5% of the microbiome), complementary to our study that found *Actinobacteria* to be a minor but consistent contributor to the community across the depth gradient, composing ~ 1–6% of the microbiome. However, in contrast to Olson and Gao (2013), we did find a depth-related decline in the abundance of *Cyanobacteria*-related sequences and an increase in the abundance of *Chloroflexi* at LC, suggesting that flexibility among autotrophic and mixotrophic sponge associates may shift their populations in order to maintain a consistent nutritional benefit to the host, although we also found

that the relative abundances of both *Cyanobacteria*- and *Chloroflexi*-related sequences were less variable at LSI, perhaps due to greater supplemental nutrient enrichment with depth in addition to the well-documented increases in particulate food availability with depth (Lesser, 2006; Trussell *et al*., 2006; Lesser and Slattery, 2013), resulting in less reliance on nutritional support from their microbial symbionts.

This study has documented the stability of core members of the *X. muta* microbiome, even as significant shifts in resources (e.g. irradiance, temperature, nutrients) occur from 10 to 91 m. Relative abundance among core residents shifted across the mesophotic depth gradient at LC, primarily driven by a reduction in *Cyanobacteria*. However, sponges at LSI demonstrated a stable community (composition and abundance) across the depth range sampled. We hypothesize that a concurrent increase in nutrients with depth may have supported a more stable microbial community at LSI in comparison to LC. This study supports previous research on the community structure of sponge microbiomes (Schmitt *et al*., 2008, 2012; Olson and Gao, 2013), and provides additional evidence that *X. muta* sponges support highly diverse, stable and species-specific microbial communities. However, our results also demonstrate that holobiont community structure retains some flexibility when faced with significant resource challenges, potentially allowing hosts to adapt to changing environmental stressors by taking advantage of the natural refugia found at mesophotic depths. These results demonstrate the critical need to examine species from multiple geographic locations, in addition to collecting relevant abiotic and biotic environmental measurements, when making hypotheses about holobiont community relationships.

Experimental procedures

Sample collection and processing

Replicate samples of *Xestospongia muta* were collected using open circuit technical diving along a 10–90 m depth gradient at two locations: Rock Bottom Reef, Little Cayman, Cayman Islands (LC) (19° 42′7.36″ N, 80° 3′24.94′ W), and North Perry Reef, Lee Stocking Island, Bahamas (LSI) (23° 47′0.03″ N, 76° 6′5.14″ W) in the Spring of 2008 and 2009 respectively. The microbial community was analysed using 454 pyrosequencing of the16S rRNA gene, a conserved taxonomic marker for bacterial and archaeal community analyses from environmental DNA (i.e. metagenetics; Creer *et al*., 2010, Boudouresque, 2011, Esposito and Kirschberg, 2014). At LC, sponge samples ($n = 3$ each depth) were collected from 10, 18, 30, 46, 60 and 91 m, and at LSI sponge samples ($n = 3$ each depth) were collected from 10, 15, 23, 30, 46 and 60 m. For the analyses described below depths were binned into groups as follows: Shallow (= 10 m), Medium (15–23 m), Deep (30–46 m) and Very Deep (60–91 m). At each depth, a 'pie-slice' of sponge that encompassed a portion of the upper edge of the osculum and side-wall (pinacoderm and mesohyl) was collected and placed in a sterile plastic bag underwater, then placed on ice in a cooler until reaching the laboratory. All sponges were considered mature (> 0.75 m tall × 0.25–0.5 m wide) and were apparently healthy. Immediately after collection smaller representative pieces of each tissue sample were frozen for stable isotope analysis and other pieces preserved in DNA buffer (0.25M ethylenediaminetetraacetic acid [EDTA; pH 7.5], 20% dimethylsulphoxide [DMSO] and saturated sodium chloride [NaCl]; Seutin *et al*., 1991). All samples were kept frozen and transported back to the University of New Hampshire, where they were maintained at −70°C until further processing.

Seawater samples ($n = 3$, 4 l each) were collected at each depth and filtered onto 0.22 μm filters (Whatman, Piscataway, NY) and frozen in DNA buffer. The filtered seawater was analysed for nitrate and nitrite (NOx) at the Nutrient Analytical Facility at Woods Hole Oceanographic Institute (Woods Hole, MA, USA) for analysis using a Lachat QuikChem 8000 (flow injection analysis system) according to standard protocols. Temperature (°C) and irradiance (μmol quanta m^{-2} s^{-1}) profile measurements ($n = 5$) were taken at each collection depth on several cloudless (< 10% cloud cover) days at mid-day (1200 to 1300 h) using a Seabird 19 CTD fitted with a light metre using a 4π collector that measured integrated scalar irradiance of PAR (400–700 nm). All instruments were calibrated to manufacturer's specifications. Vertical attenuation coefficients for downwelling irradiance of PAR (K_{dPAR} m^{-1}) and the optical depths for 1% and 10% irradiances were calculated as described by Kirk (1994).

Natural stable isotope analyses

After transport to the University of New Hampshire, subsamples from each sponge were freeze-dried and acidified to remove residual carbonates and processed for bulk stable isotopic analyses at the Marine Biological Laboratory (Woods Hole, MA). Samples were analysed for particulate C and N, as well as the natural abundance of the stable isotopes $\delta^{15}N$ and $\delta^{13}C$ using a Europa ANCA-SL elemental analyser-gas chromatograph attached to a continuous-flow Europa 20-20 gas source stable isotope ratio mass spectrometer. The analytical precision of the instrument is ± 0.1‰, and the mean precision of sample replicates for $\delta^{13}C$ was ± 0.4 ‰ and $\delta^{15}N$ was ± 0.2 ‰. The carbon isotope results are reported relative to Vienna Pee Dee Belemnite, and the nitrogen isotope results are reported relative to atmospheric air, and both are expressed using the delta (δ) notation in units per mil (‰).

DNA extraction

Genomic DNA was extracted from preserved sponge samples using a hexadecyltrimethylammonium bromide (CTAB) procedure as in Fiore and colleagues (2013a,b). Briefly, sponges were placed in 600 μl of 2X CTAB mixture (Tris, pH 8.0 [0.0121 g ml^{-1}], NaCl [0.0818 g ml^{-1}], EDTA [0.00744 g ml^{-1}], CTAB [0.002 g ml^{-1}]) and homogenized with a pestle followed by brief sonication. Proteinase K (5 μl of 20 mg ml^{-1}) was added and samples were incubated at 64°C for 3 h. An equal volume of chloroform was added to the

samples followed by centrifugation at 12 000× g for 10 min. DNA was precipitated with equal volumes of 100% ethanol, followed by two washes with 70% ethanol. Extractions were checked for quality and concentration using a NanoDrop spectrophotometer (2000c, Thermo Fisher, Waltham, MA). In some cases, a phenol : chloroform : isoamyl alcohol (25:24:1) extraction was performed to further clean the samples.

Metagenetic 16S rRNA gene pyrosequencing

All samples were polymerase chain reaction (PCR)-amplified with universal primers designed to amplify Bacteria and Archaea (hypervariable V6 region), consisting of the forward primer U789F (5′-TAGATACCCSSGTAGTCC-3′) and the reverse primer U1068R (5′-CTGACGRCRGCCATGC-3′; Baker *et al*., 2003, Lee *et al*., 2010). Three PCR reactions of 25 µl were performed for each sample and pooled prior to electrophoresis. The PCR consisted of 0.25 µl of 50X Titanium Taq polymerase (Clontech, Mountain View, CA), 2.5 µl of 10X Titanium Taq buffer, 0.2 mmol l^{-1} dNTPs (Promega, Madison, WI), 0.4 µmol l^{-1} of each barcoded primer, and 25 ng of genomic DNA template. Reactions were performed with a thermocycler (Eppendorf Mastercycler, Wesseling-Berzdorf, Germany) using the following protocol: initial denaturation for 5 min at 95°C, 26 cycles of 95°C for 30 s, 53°C for 30 s, and 72°C for 45 s, followed by 6 min at 72°C. The PCR products were then electrophoresed on a 1% agarose gel and purified with Qiaquick gel extraction kit (Qiagen, Valencia, CA). Samples were then purified with Agencourt AMPure XP bead kit (Beckman Coulter, Danvers, MA) and quantified with a DyNA Quant 200 fluorometer (Hoefer, Holliston, MA) per manufacturer's protocol prior to combining all samples in equimolar concentration. Samples were pyrosequenced on the ROCHE/454 GS FLX+ platform (Roche, Branford, CT) at the University of Illinois W.M. Keck Center for Comparative and Functional Genomics (Urbana-Champaign, IL).

Sequence processing and statistical analysis

Sequences were processed through the Quantitative Insights into Microbial Ecology (QIIME) pipeline v 1.9.1 (Caporaso *et al*., 2010). Briefly, sequences of length < 200 bp with ambiguous base calls or homopolymer runs exceeding 8 bp were removed. Sequences were aligned against the August 2013 curated Greengenes database (gg_13_8_otus; http://greengenes.secondgenome.com/ alignment; Altschub *et al*., 1997; DeSantis *et al*., 2006; Pruesse *et al*., 2007) as a reference. Operational taxonomic units were defined using PyNAST (Caporaso *et al*., 2010) after removal of singleton sequences (Behnke *et al*., 2011) and clustering at 3% divergence (97% similarity). Chimeric artefacts were also removed using UCHIME (Edgar *et al*., 2011). The OTUs were taxonomically classified using a BLAST-based method against the August 2013-curated Greengenes database (see above), and compiled at each taxonomic level into a counts file. Any sequences that were classified as Mitochondria, Eukaryotic or Chloroplast, as well as any sequences of unknown origin, were filtered out of the dataset. Sequence counts were normalized to a proportion to account for variation in sampling depth by dividing by the total library size. The raw pyrosequencing reads were submitted to the NCBI Sequence Read Archive under BioProject Number PRJNA302303.

The OTU tables were built from QIIME-generated.biom files and pivot tables were used to construct the 'Top OTU table' as well as to condense sequences by phyla and family for further graphical interpretation in Microsoft Excel. The OTU count data were square root-transformed, and SIMPER analyses were performed to examine which depth zones and OTUs contributed most to the dissimilarity between sites. Additionally, because SIMPER analyses can be biased towards identifying small relative changes in abundant OTUs and do not provide statistical significance at the OTU level, an MGLM approach (Warton *et al*., 2012) was also employed as implemented in the R package *mvabund* (Wang *et al*., 2012). In this approach, each OTU is treated as a variable that is fitted to a separate GLM using a negative binomial distribution for the analysis of community structure between depth zone pairs. To determine which taxa contributed most to the differences between depth zones, the univariate ANOVA function in *mvabund*, which implements an analysis of deviance, was then applied to each depth zone pair using the *p.uni* argument set to return OTU-by-OTU results and adjusted to control the family-wise error rate across OTUs. Bray–Curtis distance matrices were built to examine additional patterns of community structure and visualized using principal coordinate analyses (PCoA). Pearson correlation vectors were overlaid to demonstrate which taxa have strong positive or negative correlations with either PCoA axis, indicative of depth differences. A PERMANOVA (using 10 000 permutations) determined whether spatial separation between depth (i.e. Shallow, Medium, Deep, Very Deep) for each site was statistically significant. The above multidimensional statistical analyses were performed in PRIMER V7 with the PERMANOVA+ add-on (PRIMER-E, Devon, UK). The CCA was conducted to examine the influence of environmental drivers on community shifts using the vegan package (Oksanen *et al*., 2015) in R (R Core Team, 2015).

Acknowledgements

This work was conducted at the Little Cayman Research Centre and the Caribbean Marine Research Center. Marc Slattery and Elizabeth Kintzing provided technical diving support, and Jessica Jarett helped with both field and laboratory support. Additional statistical help was provided by Mr. Jordan Ramsdell (UNH), Mr. Stephen Sefick (Auburn University) and Dr. Sabrina Pankey (UNH). All experiments conducted for this study complied with the laws of the Cayman Islands, Bahamas and the United States of America. This project was funded by grants from NOAA's National Institute for Undersea Science and Technology (14U752) and the National Science Foundation (IOS 1231468). The views expressed herein are those of the authors and do not necessarily reflect the views of these agencies.

References

Altschub, S.F., Madden, T.L., Schäffer, A.A., Zhang, J., Zhang, Z., Miller, W., and Lipman, D.J. (1997) Gapped BLAST and PSI-BLAST: a new generation of protein database search programs. *Nucleic Acid Res* **25:** 3389–3402.

Aronson, R.B., Precht, W., Toscano, M., and Koltes, K.H. (2002) The 1998 bleaching event and its aftermath on a coral reef in Belize. *MarBiol* **141:** 435–447.

Baker, G.C., Smith, J.J., and Cowan, D.A. (2003) Review and re-analysis of domain-specific 16S primers. *J Microbiol Methods* **55:** 541–555.

Behnke, A., Engel, M., Christen, R., Nebel, M., Klein, R.R., and Stoeck, T. (2011) Depicting more accurate pictures of protistan community complexity using pyrosequencing of hypervariable SSU rRNA gene regions. *Environ Microbiol* **13:** 340–349.

Bell, J.J. (2008) The functional roles of marine sponges. *Est Coast Shelf Sci* **79:** 341–353.

Bell, J.J., Davy, S.K., Jones, T., Taylor, M.W., and Webster, N.S. (2013) Could some coral reefs become sponge reefs as our climate changes? *Glob Change Biol* **19:** 2613–2624.

Bongaerts, P., Ridgway, T., Sampayo, E.M., and Hoegh-Guldberg, O. (2010) Assessing the 'deep reef refugia' hypothesis: focus on Caribbean reefs. *Coral Reefs* **2:** 309–327.

Boudouresque, C.F. (2011) Taxonomy and phylogeny of unicellular eukaryotes. In *Environmental Microbiology: Fundamentals and Applications: Microbial Ecology*. Bertrand, J.C., Caumette, P., Lebaron, P., Matheron, R., Normand, P., and Sime-Ngando, T. (eds). Springer Dordrecht Heidelberg New York London: Springer Press, pp. 193–194.

Brazeau, D.A., Lesser, M.P., and Slattery, M. (2013) Genetic structure in the coral, *Montastraea cavernosa*: assessing genetic differentiation among and within mesophotic reefs. *PLoS ONE* **8:** e65845.

Caporaso, J.G., Kuczynski, J., Stombaugh, J., Bittinger, K., Bushman, F.D., Costello, E.K., *et al*. (2010) QIIME allows analysis of high-throughput community sequencing data. *Nat Methods* **7:** 335–336.

Colvard, N.B., and Edmunds, P.J. (2011) Decadal-scale changes in abundance of non-scleractinian invertebrates on a Caribbean coral reef. *J Exp Mar Biol Ecol* **397:** 153–160.

Corredor, J.E., Wilkinson, C.R., Vicente, V.P., Morell, J.M., and Otero, E. (1988) Nitrate release by Caribbean reef sponges. *Limnol Oceanogr* **33:** 114–120.

Creer, S., Fonseca, V.G., Porazinska, D.L., Giblin-Davis, R.M., Sung, W., Power, D.M., *et al*. (2010) Ultrasequencing of the meiofaunal biosphere: practice, pitfalls and promises. *Molec Ecol* **19** (Suppl. 1): 4–20.

DeSantis, T.Z., Hugenholtz, P., Larsen, N., Rojas, M., Brodie, E.L., Keller, K., *et al*. (2006) Greengenes, a chimera-checked 16S rRNA gene database and workbench compatible with ARB. *Appl Environ Microbiol* **7:** 5069–5072.

Diaz, M.C., and Rutzler, K. (2001) Sponges: an essential component of Caribbean coral reefs. *Bull Mar Sci* **69:** 535–546.

Edgar, R.C., Haas, B.J., Clemente, J.C., Quince, C., and Knight, R. (2011) UCHIME improves sensitivity and speed of chimera detection. *Bioinformatics* **27** (16): 2194–2200.

Erwin, P.M., and Thacker, R.W. (2008a) Cryptic diversity of the symbiotic cyanobacterium *Synechococcus spongiarum* among sponge hosts. *Mol Ecol* **17:** 2937–2947.

Erwin, P.M., and Thacker, R.W. (2008b) Phototrophic nutrition and symbiont diversity of two Caribbean sponge-cyanobacteria symbioses. *Mar Ecol Prog Ser* **362:** 139–147.

Esposito, A., and Kirschberg, M. (2014) How many 16S-based studies should be included in a metagenomic conference? It may be a matter of etymology. *FEMS Microbiol Lett* **351:** 145–146.

Fiore, C.L., Jarett, J.K., Olson, N.D., and Lesser, M.P. (2010) Nitrogen fixation and nitrogen transformations in marine symbioses. *Trends Microbiol* **18:** 455–463.

Fiore, C.L., Baker, D.M., and Lesser, M.P. (2013a) Nitrogen biogeochemistry in the Caribbean sponge, *Xestospongia muta*: a source or sink of dissolved inorganic nitrogen? *PLoS ONE* **8:** e72961.

Fiore, C.L., Jarett, J.K., and Lesser, M.P. (2013b) Symbiotic prokaryotic communities from different populations of the giant barrel sponge, *Xestospongia muta*. *Microbiol Open* **2:** 938–952.

Fiore, C.L., Labrie, M., Jarett, J.K., and Lesser, M.P. (2015) Transcriptional activity of the giant barrel sponge, *Xestospongia muta* holobiont: molecular evidence for metabolic interchange. *Front Microbiol* **6:** 364.

Gardner, T.A., Cote, I.M., Gill, J.A., Grant, A., and Watkinson, A.R. (2003) Long-term region-wide declines in Caribbean corals. *Science* **301:** 958–960.

Hentschel, U., Piel, J., Degnan, S.M., and Taylor, M.W. (2012) Genomic insights into the marine sponge microbiome. *Nature Reviews Microbiol* **10:** 641–654.

Hochmuth, T., Niederkruger, H., Gernert, C., Siegl, A., Taudien, S., Platzer, M., *et al*. (2010) Linking chemical and microbial diversity in marine sponges: possible role for Poribacteria as producers of methyl-branched fatty acids. *Chembiochem* **11:** 2572–2578.

Kahng, S.E., Copus, J.M., and Wagner, D. (2014) Recent advances in the ecology of mesophotic coral reef ecosystems (MCEs). *Curr Opin Environ Sustain* **7:** 72–81.

Kirk, J.T.O. (1994) *Light and Photosynthesis in Aquatic Ecosystems*. London: Cambridge University Press.

Lee, O.O., Wang, Y., Yang, J., Lafi, F.F., Al-Suwailem, A., and Qian, P.-Y. (2010) Pyrosequencing reveals highly diverse and species-specific microbial communities in sponges from the Red Sea. *ISME J* **5:** 650–664.

Lesser, M.P. (2006) Benthic-pelagic coupling on coral reefs: feeding and growth of Caribbean sponges. *J Exp Mar Biol Ecol* **328:** 277–288.

Lesser, M.P., and Slattery, M. (2013) Ecology of Caribbean sponges: are top-down or bottom-up processes more important? *PLoS ONE* **8:** e79799.

Lesser, M.P., Slattery, M., and Leichter, J.J. (2009) Ecology of mesophotic coral reefs. *J Exp Mar Biol Ecol* **375:** 1–8.

Lesser, M.P., Slattery, M., Stat, M., Ojimi, M., Gates, R.D., and Grottoli, A. (2010) Photoacclimatization by the coral *Montastraea cavernosa* in the mesophotic zone: light, food, and genetics. *Ecology* **91:** 990–1003.

Lindell, D., Penno, S., Al-Qutob, M., David, E., Rivlin, T., Lazar, B., and Post, A.F. (2005) Expression of the nitrogen stress response gene *ntcA* reveals nitrogen-sufficient *Synechoccocus* populations in the oligotrophic northern Red Sea. *Limnol Oceanogr* **50:** 1932–1944.

Liu, Z., Klatt, C.G., Wood, J.M., Rusch, D.B., Ludwig, M., Wittekindt, N., *et al*. (2011) Metatranscriptomic analysis of chlorophototrophs of a hot-spring microbial mat. *ISME J* **5:** 1279–1290.

Lopez-Victoria, M., Zea, S., and Weil, E. (2006) Competition for space between encrusting excavating Caribbean sponges and other coral reef organisms. *Mar Ecol Prog Ser* **312:** 113–121.

McMurray, S.E., Henkel, T.P., and Pawlik, J.R. (2010) Demographics of increasing populations of the giant barrel sponge *Xestospongia muta* in the Florida Keys. *Ecology* **91:** 560–570.

Maldonado, M., Ribes, M., and van Duyl, F.C. (2012) Nutrient fluxes through sponges: biology, budgets, and ecological implications. *Adv Mar Biol* **62:** 113–182.

Mohamed, N.M., Colman, A.S., Tal, Y., and Hill, R.T. (2008) Diversity and expression of nitrogen fixation genes in bacterial symbionts of marine sponges. *Env Microbiol* **10:** 2910–2921.

Montalvo, N.F., Mohamed, N.M., Enticknap, J.J., and Hill, R.T. (2005) Novel actinobacteria from marine sponges. *Antonie Van Leeuwenhoek* **87:** 29–36.

Morrow, K.M., Bourne, D.G., Humphrey, C., Botté, E.S., Laffy, P., Zaneveld, J., *et al*. (2014) Natural volcanic CO_2 seeps reveal future trajectories for host-microbial associations in corals and sponge. *ISME J* **9:** 894–908.

Oksanen, J., Guillaume Blanchet, F., Kindt, R., Legendre, P., Minchin, P.R., O'Hara, R.B., *et al*. (2015) vegan: Community Ecology Package. R package version 2.3-0. http://CRAN.R-project.org/package=vegan.

Olson, J.B., and Gao, X. (2013) Characterizing the bacterial associates of three Caribbean sponges along a gradient from shallow to mesophotic depths. *FEMS Microbiol Ecol* **85:** 74–84.

Olson, J.B., and Kellogg, C.A. (2010) Microbial ecology of corals, sponges, and algae in mesophotic coral environments. *FEMS Microbiol Ecol* **73:** 17–30.

Pawlik, J.R. (2011) The chemical ecology of sponges on Caribbean reefs: natural products shape natural systems. *Bioscience* **61:** 888–898.

Porter, J.W., and Targett, N.M. (1988) Allelochemical interactions between sponges and corals. *Biol Bull* **175:** 230–239.

Pruesse, E., Quast, C., Knittel, K., Fuchs, B.M., Ludwig, W., Peplies, J., and Glöckner, O. (2007) SILVA: a comprehensive online resource for quality checked and aligned ribosomal RNA sequence data compatible with ARB. *Nucleic Acids Res* **35:** 7188–7196.

R Core Team (2015) *R: A Language and Environment for Statistical Computing*. Vienna, Austria: R Foundation for Statistical Computing. URL http://www.R-project.org/.

Randall, J.E., and Hartman, W.D. (1968) Sponge-feeding fishes of the West Indies. *Mar Biol* **1:** 216–225.

Reed, J.K., and Pomponi, S.A. (1997) Biodiversity and distribution of deep and shallow water sponges in the Bahamas. *Proc 8th Int Coral Reef Symp* **2:** 1387–1392.

Reveillaud, J., Maignien, L., Eren, A.M., Huber, J.A., Apprill, A., Sogin, M.L., and Vanreusel, A. (2014) Host-specificity among abundant and rare taxa in the sponge microbiome. *ISME J* **8:** 1198–1209.

Schmitt, S., Angermeier, H., Schiller, R., Lindquist, N., and Hentschel, U. (2008) Molecular microbial diversity survey of sponge reproductive stages and mechanistic insights into vertical transmission of microbial symbionts. *Appl Environ Microbiol* **74:** 7694–7708.

Schmitt, S., Deines, P., Behnam, F., Wagner, M., and Taylor, M.W. (2011) *Chloroflexi* bacteria are more diverse, abundant, and similar in high than in low microbial abundance sponges. *FEMS Microbiol Ecol* **78:** 497–510.

Schmitt, S., Tsai, P., Bell, J., Fromont, J., Ilan, M., Lindquist, N., *et al*. (2012) Assessing the complex sponge microbiota: core, variable, and species-specific bacterial communities in marine sponges. *ISME J* **6:** 564–576.

Seutin, G., White, B.N., and Boag, P.T. (1991) Preservation of avian blood and tissue samples for DNA analyses. *Can J Zool* **69:** 82–90.

Siegl, A., and Hentschel, U. (2010) PKS and NRPS gene clusters from microbial symbiont cells of marine sponges by whole genome amplification. *Environ Microbiol Rep* **2:** 507–513.

Siegl, A., Kamke, J., Hochmuth, T., Piel, J., Richter, M., Liang, C., *et al*. (2011) Single-cell genomics reveals the lifestyle of *Poribacteria*, a candidate phylum symbiotically associated with marine sponges. *ISME J* **5:** 61–70.

Slattery, M., and Gochfeld, D.J. (2012) Chemically mediated competition and host–pathogen interactions among marine organisms. In *Handbook of Marine Natural Products*. Fattorusso, E., Gerwick, W.H., and Taglialatela-Scafati, O. (eds). New York: Springer, pp. 824–859.

Slattery, M., and Lesser, M.P. (2014) Allelopathy in the tropical alga *Lobophora variegata*: mechanistic basis for a phase shift on mesophotic coral reefs. *J Phycol* **50:** 493–505.

Slattery, M., Lesser, M.P., Brazeau, D., Stokes, M.D., and Leichter, J.J. (2011) Connectivity and stability of mesophotic coral reefs. *J Exp Mar Biol Ecol* **408:** 32–41.

Slattery, M., Gochfeld, D.J., Diaz, M.C., Thacker, R.W., and Lesser, M.P. (2015) Variability in chemical defense across a shallow to mesophotic depth gradient in the Caribbean sponge *Plakortis angulospiculatus*. *Coral Reefs* doi:10.1007/s00338-015-1324-9.

van Soest, R.W., Boury-Esnault, N., Vacelet, J., Dohrmann, M., Erpenbeck, D., De Voogd, N.J., *et al*. (2012) Global diversity of sponges (Porifera). *PLoS ONE* **7:** e35105.

Southwell, M.W., Weisz, J.B., Martens, C.S., and Lindquist, N. (2008) *In situ* fluxes of dissolved inorganic nitrogen from the sponge community on Conch Reef, Key Largo, Florida. *Limnol Oceanogr* **53:** 986–996.

Steindler, L., Hucheon, D., Avni, A., and Ilan, M. (2005) 16S rRNA phylogeny of sponge associated cyanobacteria. *Appl Environ Microbiol* **71:** 4127–4131.

Taylor, M.W., Radax, R., Steger, D., and Wagner, M. (2007) Sponge-associated microorganisms: evolution, ecology, and biotechnological potential. *Microbiol Mol Biol Rev* **71:** 295–347.

Thacker, R.W., and Freeman, C.J. (2012) Sponge-microbe symbioses: recent advances and new directions. *Adv Mar Biol* **62:** 57–112.

Trussell, G.C., Lesser, M.P., Patterson, M.R., and Genovese, S.J. (2006) Depth-specific differences in growth of the reef sponge *Callyspongia vaginalis*: role of bottom-up effects. *Mar Ecol Prog Ser* **323:** 149–158.

Wang, Y., Naumann, U., Wright, S.T., and Warton, D.I. (2012) mvabund–an R package for model-based analysis of multivariate abundance data. *Meth Ecol Evol* **3:** 471–474.
Warton, D.I., Wright, S.T., and Wang, Y. (2012) Distance-based multivariate analyses confound location and dispersion effects. *Meth Ecol Evol* **3:** 89–101.
Wilkinson, C.R. (1983) Net primary productivity in coral reef sponges. *Science* **219:** 410–412.
Wulff, J.L. (1984) Sponge-mediated coral reef growth and rejuvenation. *Coral Reefs* **3:** 157–163.
Wulff, J.L. (2006) Ecological interactions of marine sponges. *Can J Zool* **84:** 146–166.
Wulff, J. (2012) Ecological interactions and the distribution, abundance, and diversity of sponges. *Adv Mar Biol* **61:** 273–344.
Zhang, F., Blasiack, L.C., Karolin, J.O., Powell, R.J., Geddes, C.D., and Hill, R.T. (2015) Phosphorous sequestration n the form of polyphosphate by microbial symbionts in marine sponges. *Proc Natl Acad Sci* **112:** 4381–4386.

Supporting information

Additional Supporting Information may be found in the online version of this article at the publisher's web-site:

Fig. S1. Rarefaction curve for each depth zone generated in QIIME using alpha_rarefaction.py.
Table S1. PERMANOVA with pairwise comparisons for (A) Little Cayman and (B) Lee Stocking Island.
Table S2. (A) Similarity percentage analysis (SIMPER) for two most significant operational taxonomic units (OTUs) driving differences between the depth range pairs at Little Cayman. (B) Multiple generalized linear models (MGLM) for all pairwise comparisons at Little Cayman. All significantly contributing OTUs are reported for each pair. Significant pairwise comparisons were not detected at Lee Stocking Island and are not reported.
Table S3. OTUs that composed principal coordinate analysis (PCoA) clusters 13 and 38 from the Little Cayman (LC) dataset.